A Donor-Acceptor Indenoperylene Dye for Highly Efficient Organic Dye-Sensitized Solar Cells.

ARTICLE *in* JOURNAL OF THE AMERICAN CHEMICAL SOCIETY · MARCH 2015

Impact Factor: 12.11 · DOI: 10.1021/jacs.5b01537 · Source: PubMed

6 AUTHORS, INCLUDING:

Min Zhang
Chinese Academy of Sciences
39 PUBLICATIONS **2,078** CITATIONS
SEE PROFILE

Lin Yang
China University of Geosciences (Beijing)
34 PUBLICATIONS **243** CITATIONS
SEE PROFILE

Renzhi Li
Chinese Academy of Sciences
30 PUBLICATIONS **1,878** CITATIONS
SEE PROFILE

Peng Wang
Beijing University of Civil Engineering and Arc…
741 PUBLICATIONS **17,608** CITATIONS
SEE PROFILE

JACS
JOURNAL OF THE AMERICAN CHEMICAL SOCIETY
Communication
pubs.acs.org/JACS

Donor/Acceptor Indenoperylene Dye for Highly Efficient Organic Dye-Sensitized Solar Cells

Zhaoyang Yao,[†,‡] Min Zhang,[†] Heng Wu,[†] Lin Yang,[†,‡] Renzhi Li,[†] and Peng Wang*[,†]

[†]State Key Laboratory of Polymer Physics and Chemistry, Changchun Institute of Applied Chemistry, Chinese Academy of Sciences, Changchun 130022, China

[‡]University of Chinese Academy of Sciences, Beijing 100049, China

Supporting Information

ABSTRACT: An *N*-annulated indenoperylene electron-donor decorated with photochemically inactive segments is synthesized and further conjugated via triple bond with electron-acceptor benzothiadiazolylbenzoic acid for a metal-free donor/acceptor dye. Without use of any coadsorbate, the judiciously tailored indenoperylene dye achieves a high-power conversion efficiency of 12.5% under irradiance of 100 mW cm^{-2} AM1.5G sunlight.

In the global motif of sustainable development, massive research endeavors have been devoted to dye-sensitized solar cells (DSCs)[1] with the aim of eco-friendly and low-cost converting of solar energy to clean electricity. Apart from carrier transporters, the self-assembled layer of dye molecules on the surface of titania in DSCs largely regulates the yield of harnessed solar photons and separated charges, dominating the final power output.[2] From the viewpoints of stability and efficiency, a few ruthenium polypyridine[3] and zinc porphyrin[4] complexes are the hitherto best-performing dyes for DSCs. However, ruthenium dyes own the obvious dilemma of resource scarcity and heavy metal toxicity; zinc poryphyrin dyes have the painful obstacles of low synthetic yield and handling of highly toxic chemicals (e.g., thiophosgene and 2,3-dichloro-5,6-dicyano-1,4-benzoquinone). Attention has also been drawn to metal-free organic dyes because of abundant raw materials, adjustable molecular designs, and cheerful vision effects.[5] Although a zinc porphyrin dye has already reached a power conversion efficiency (PCE) of 13%,[4d] thus far only a few donor/acceptor (D/A) organic dyes have achieved over 11% PCE.[6,7] Two years ago, we employed benzothiadiazolylbenzoic acid (BTBA) as electron-acceptor for a low-energy-gap organic dye with an 11.5% PCE.[6] Later, Kakiage[7] and his co-workers reported an alkoxysilyl carbazole dye by modifying seminal dye **MK-2**[8] (Figure S1) to reach an over 12% PCE for organic DSCs. Both organic dyes needed to be coupled with some photovoltage-enhancing coadsorbates, in either one or two steps, to attain a high efficiency.

Organic small molecules derived from a coplanar perylene skeleton are ordinarily endowed with a high molar absorption coefficient, large luminescence yield, and attractive photostability, promoting their extensive utilizations as fluorescent probes, light-emitting materials, and paints/pigments.[9] Meanwhile, perylene has been pursued as a polycyclic aromatic hydrocarbon (PAH) module of metal-free organic DSC dyes, but most of them have disappointing PCEs.[10] Luo et al.[11] used a phenyl-functionalized *N*-annulated perylene (PNP) as the electron-donor for low-energy-gap zinc porphyrin dye **WW6** (Figure S1) with a PCE of 10.5%, comparable to that of structurally simpler benchmark dye **YD2-*o*-C8**[4b] (Figure S1) because of fast interfacial charge recombination. More recently, we slightly modified the PNP[11] electron-donor with bulkier photochemically idle substitutents and conjugated it with an ethynylbenzothiadiazolylbenzoic acid (EBTBA) electron-acceptor[4c,d,10q] to prepare simple perylene dye **C272** (Figure 1) with a PCE of 10.4%.[12]

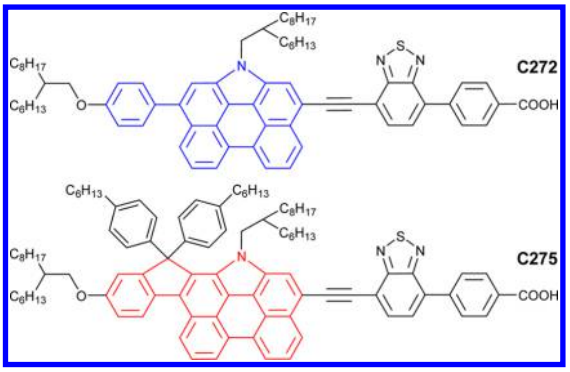

Figure 1. Chemical structures of perylene dyes **C272** and **C275** with EBTBA as electron-acceptor. PNP and NIP are displayed in blue and red, respectively.

Bearing in mind our prior studies[13] on synchrously enhanced light absorption and photovoltage of D/A dyes via rigidifying aromatic units with cyclopentadiene, here we envisage a coplanar, electron-rich PAH, *N*-annulated indeno[2,1-*b*]-perylene (NIP, Figure 1). In our design of metal-free D/A dye **C275** with electron-acceptor EBTBA, the insoluble rigid segment of NIP is end-capped with one branched 2-hexyldecyloxy and side-tethered with 2-hexyldecyl and hexylphenyl principally to abate strong intermolecular π/π stacking. Dye aggregation is generally considered to have an adverse effect on carrier photogeneration because of excited-state annihilation.[4,14] Without any coadsorbate, judiciously tailored **C275** derived from NIP can be used alone to make a DSC with an impressive PCE of 12.5% under 100 mW cm^{-2} air mass global (AM1.5G) conditions.

Received: February 11, 2015
Published: March 5, 2015

DOI: 10.1021/jacs.5b01537
J. Am. Chem. Soc. 2015, 137, 3799−3802

Scheme S1 outlines the synthetic route to **C275**. We first executed an almost quantitative alkylation of 2-bromo-5-hydroxybenzaldehyde (**1**)[15] with 2-hexyldecyl 4-methylbenzenesulfonate[16] as the alkylating regent to obtain 2-bromo-5-((2-hexyldecyl)oxy)benzaldehyde (**2**), which was then slowly but almost quantitatively oxidized with Jones reagent to form 2-bromo-5-((2-hexyldecyl)oxy)benzoic acid (**3**). Next, **3** was completely transformed into ester **4**. Further implementation of Pd-catalyzed Miyaura borylation under mild conditions converted **4** to phenylboronic acid pinacol ester **5** in excellent yield. Subsequent Suzuki-Miyaura cross-coupling of **5** and 3-bromo-1-(2-hexyldecyl)-1*H*-phenanthro[1,10,9,8-*cdefg*]-carbazole[17] produced key intermediate **6** in good yield. Then, **6** was implemented in a carbonyl addition reaction with (4-hexylphenyl)magnesium bromide[13b] to generate a tertiary alcohol, which was not isolated and underwent intramolecular Friedel-Crafts cyclization with the aid of solid acid catalyst Amberlyst 15 to afford coplanar electron-donor **7**. Later, we performed regioselective monobromination of **7** with *N*-bromosuccinimide at a relatively low temperature to get **8** in excellent yield, which was further cross-coupled with butyl 4-(7-ethynylbenzo[*c*][1,2,5]thiadiazol-4-yl)benzoate[10q] via the Sonogashira reaction to generate dye precursor **9**. Compound **9** was subjected to hydrolysis with KOH as catalyst, and the hydrolyzate was carefully acidified with a dilute aqueous solution of phosphoric acid to afford the desired dye.

Electrochemical behavior of THF solutions was then measured to assess approximately the influences of electron-donors (NIP vs PNP) on the HOMO and LUMO energy levels. From the low-sweep-rate cyclic voltammograms (Figure 2a) with decamethylferrocene (DMFC) as internal reference, energy levels (Table S1) were viably derived via the equation $E = -4.88 - eE_{onset}$, where E_{onset} is the onset potential of reduction or oxidation of a ground-state dye. For **C272** and **C275**, the electron-donor alteration from PNP to NIP does not exert a perceivable effect on the LUMO energy level (E_L^{CV}), but rather significantly destabilizes the HOMO energy level (E_H^{CV}) by 100 meV, giving rise to a narrower LUMO/HOMO energy gap ($\Delta E_{L/H}^{CV}$, 1.76 and 1.86 eV for **C275** and **C272**, respectively). Thus, we observed a 24 nm redshift of maximum absorption wavelength (λ_{MAX}^{EA}, Figure 2b). The use of a rigidified electron-donor (NIP vs PNP) also brings forth an improved maximum molar absorption coefficient (ε_{MAX}^{EA}, 51.1×10^3 versus 36.1×10^3 M^{-1} cm^{-1} for **C275** vs **C272**).

As listed in Table S1, the relative positioning of LUMO and HOMO as well as the red-shifting of λ_{MAX}^{EA} can be nicely reproduced by density functional theory (DFT) and time-dependent DFT calculations at the levels of B3LYP/6-311G(d,p)[18] and TD-MPW1K/6-311G(d,p),[19] respectively. The conductor-like polarized continuum model (C-PCM) was picked for the simulation of solvent effects of THF.[20] In general, the $S_0 \rightarrow S_1$ vertical electronic transitions to LUMO for both EBTBA-based perylene dyes are 92% originated from HOMO, displaying a feature of intramolecular charge-transfer easily apprehended from the contour plots of molecular orbitals (Figure 2c). The HOMO and LUMO energy levels of PNP, NIP, and EBTBA were also computed to disclose their underlying correlations with those of **C272** and **C275**. For both dyes, their LUMO energy levels are mostly inherited from that of the common electron-acceptor EBTBA, whereas their HOMO energy levels in general match those of their respective electron-donors (Figure 2d).

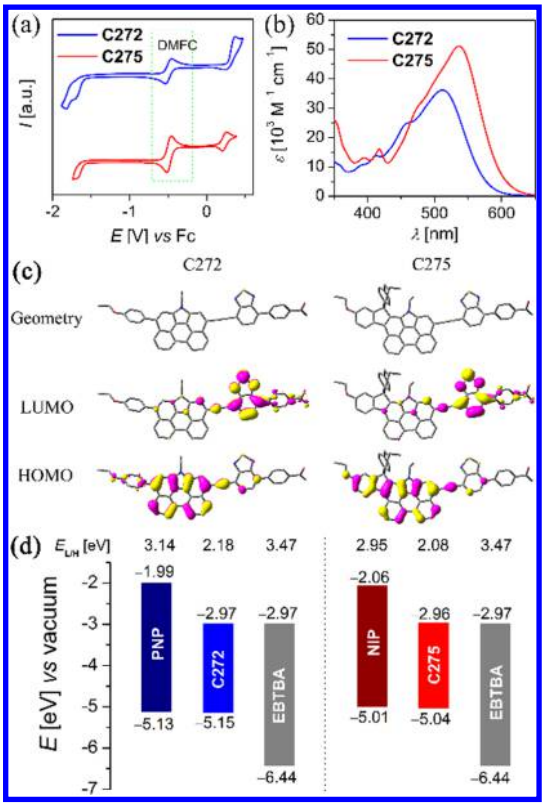

Figure 2. (a) Cyclic voltammograms of perylene dyes **C272** and **C275** dissolved in THF with 1-ethyl-3-methylimidazolium bis-(trifluoromethanesulfonyl)imide as supporting electrolyte. Potential sweep rate = 5 mV s^{-1}. DMFC was added as internal reference, and all potentials are further calibrated with respect to ferrocen. (b) Electronic absorption spectra of dyes dissolved in THF (10 μM). (c) Cantor plots of molecular orbitals involved in the $S_0 \rightarrow S_1$ transitions. Large aliphatic substituents were replaced with ethyl to improve computational efficiency. (d) Energy gaps ($\Delta E_{L/H}$), LUMO energy levels (values above color bars), and HOMO energy levels (value under color bars) of dye molecules and their electron donating and accepting segments.

To check whether the change of dye molecules would affect electron-injection yield (ϕ_{EI}), we performed time-correlated single photon counting (TCSPC) experiments and monitored the variation of photoluminescence (PL) of dyed alumina and titania films.[21] To make our PL measurements closely relate to the operation of real DSCs discussed later, all films were infiltrated with a Co-phen electrolyte[22] (recipe described in the Supporting Information) for cell fabrication. We consider that alumina is incapable of accepting electrons from these two perylene dyes in the electronically excited-states (D*); thus, PL traces (blue curves) in Figure S2 are associated with radiative and radiationless deactivation of D*. The dislodgement of the Co-phen redox couple does not tune PL traces at all, indicating that charge and energy transfers between D* and the redox couple do not occur. Obviously, reductive quenching is dynamically inhibited despite it being energetically allowed. The absence of Förster resonance energy transfer is intrinsically allied to the larger HOMO/LUMO gaps of the Co-phen redox couple compared to these two perylene dyes.

Upon replacement of alumina with titania, significant PL quenching (PLQ) is easily seen in Figure S2. PLQ provides indirect evidence of the occurrence of charge separation at the energy-offset titania/dye interface, although electron injection could be directly probed with ultrafast midinfrared spectrosco-

DOI: 10.1021/jacs.5b01537
J. Am. Chem. Soc. 2015, 137, 3799−3802

py.[23] The areas under the time-correlated PL traces (Figure S2) were further plotted using integration to roughly estimate ϕ_{EI} (96% for both dyes). The almost quantitative electron injection is supported by a high percentage of chemical bonding of **C272** and **C275** on the surface of titania, as revealed by ATR-FTIR spectra (Figure S3). The fact that a very minor quantity of dye molecules does not inject electrons to titania could be ascribed to dynamic competition between the electron-injection process and other excited-state deactivation events.

As shown in Figure 3b, the external quantum efficiencies (EQEs) of DSCs made with bilayer dye-grafted titanium films

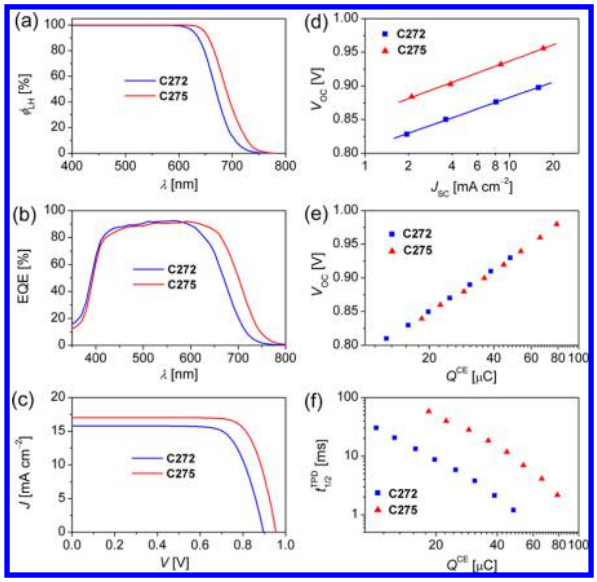

Figure 3. (a) Plots of light-harvesting yield (ϕ_{LH}) vs wavelength (λ) for 8.0 μm thick dye-grafted mesoporous titania films immersed in a Co-phen electrolyte. (b) Plots of external quantum efficiency (EQE) vs λ of incident monochromatic light for cells made with dye-grafted bilayer [(5.2 + 5.0) μm thick] titania films in conjunction with a Co-phen electrolyte. (c) Current/voltage (J/V) characteristics of cells measured under an irradiance of 100 mW cm^{-2} simulated AM1.5G sunlight. Antireflection film was laminated on top of DSCs. Aperture area of metal mask was 0.160 cm^2. (d) Plots of open-circuit photovoltage (V_{OC}) vs short-circuit photocurrent density (J_{SC}). Solid lines are linear fittings. (e) Plots of charge stored in a dye-grafted titania film (Q^{CE}) vs open-circuit photovoltage (V_{OC}). (f) Comparison of electron half-lifetime ($t_{1/2}^{TPD}$) against Q^{CE}.

and Co-phen electrolyte are plotted as a function of wavelengths of incident monochromatic lights (for cell fabrication details, see the Supporting Information). The photocurrent action spectra of cells with **C272** and **C275** both exhibit a maximum of ~92%. With respect to **C272**, there is an ~40 nm red-shifting of the onset wavelength of photocurrent response for **C275**, in rough accord with ϕ_{LH} depicted in Figure 3a, owing to a narrower energy gap as well as an augmented absorption coefficient. The photocurrent density/photovoltage (J/V) curves were tested at an irradiance of 100 mW cm^{-2} simulated AM1.5G sunlight (Figure 3c). The averaged cell parameters of 12 cells made with each dye are compiled in Table 1. **C272** possesses a typical short-circuit photocurrent density (J_{SC}) of 15.81 mA cm^{-2}, an open-circuit photovoltage (V_{OC}) of 897 mV, and a fill factor (FF) of 74.4%, generating a PCE of 10.6%. In good agreement with the integrals of EQEs over the standard AM1.5G emission spectrum (ASTM G173-03), **C275** exhibits an enlarged J_{SC} value of 17.03 mA cm^{-2}, an improved V_{OC} value of 956 mV, an excellent FF of 77.0%, contributing to an ~18% improved PCE of 12.5%. It can be seen from Table 1 that under our optimized conditions, the efficiency achieved with **C275** is remarkably higher than that attained with **YD2-*o*-C8** (Figure S4).[4b]

We also recorded J/V curves at a set of light irradiances and plotted V_{OC} as a function of J_{SC} (Figure 3d). From the fitting curves, we see that at a given J_{SC} there is a ~50 mV higher V_{OC} for **C275** relative to **C272**. To examine interfacial energetic and dynamic origins of V_{OC} variation,[24] we carried out charge extraction (CE)[25] and transient photovoltage decay (TPD)[26] measurements. As shown in Figure 3e, the dye alteration from **C272** to **C275** does not affect the conduction-band edge of titania with respect to the Fermi level of Co-phen. However, at a given density of photoinjected electrons in titania, with respect to **C272**, **C275** bears a considerably elongated half lifetime ($t_{1/2}^{TPD}$) of electrons in the titania film, accounting for its enlarged photovoltage (Figure 3f). The dye loading amounts (c_m) on the mesoporous titania film were also examined with visible spectrometry (3.6×10^{-8} and 3.0×10^{-8} mol cm^{-2} μm^{-1} for **C272** and **C275**, respectively). The adverse effect[27] of a relatively lower c_m on V_{OC} is over compensated with two hexylphenyl units tethered on the sp^3 carbon of NIP in **C275**.

We have synthesized a new D/A dye, **C275**, characteristic of the new electron-donor *N*-annulated indenoperylene and electron-acceptor EBTBA. To the best of our knowledge, this is the first time that such a high PCE (12.5%) has been reached with a metal-free organic dye alone in DSCs, shedding light on further design of highly efficient dyes. Our success in the development of a powerful organic dye without use of fashionable units should stimulate further explorations of other exotic electron-releasing and -withdrawing polycyclic aromatic materials to get rid of similar material attempts and to significantly improve the efficiency of DSCs.

■ ASSOCIATED CONTENT

Supporting Information

Experimental details and additional data. This material is available free of charge via the Internet at http://pubs.acs.org.

Table 1. Averaged Photovoltaic Parameters of 12 Cells Measured under an Irradiance of 100 mW cm^{-2} Simulated AM1.5G Sunlight[a]

dye	J_{SC}^{EQE} (mA cm^{-2})	J_{sc} (mA cm^{-2})	V_{OC} (mV)	FF (%)	PCE (%)
C272	15.71 ± 0.08	15.81 ± 0.11	897 ± 4	74.4 ± 0.4	10.6 ± 0.1
C275	17.44 ± 0.05	17.03 ± 0.08	956 ± 2	77.0 ± 0.5	12.5 ± 0.1
YD2-*o*-C8	13.52 ± 0.12	14.44 ± 0.10	917 ± 7	78.3 ± 0.3	10.4 ± 0.2

[a] J_{SC}^{EQE} was derived via wavelength integration of the product of the standard AM1.5G emission spectrum (ASTM G173-03) and the EQEs measured at the short-circuit. There was a linear dependence of photocurrent on irradiance (Figure S5); we thereby evaluated the validity of measured photovoltaic parameters by comparing calculated J_{SC}^{EQE} values with experimental J_{SC} values.

DOI: 10.1021/jacs.5b01537
J. Am. Chem. Soc. 2015, 137, 3799−3802

AUTHOR INFORMATION

Corresponding Author

*peng.wang@ciac.ac.cn. Phone: 0086-431-85262952.

Notes

The authors declare no competing financial interests.

ACKNOWLEDGMENTS

This work was sponsored by the National 973 Program (2011CBA00702 and 2015CB932204) and the National Science Foundation of China (51125015, 91233206, 51473158, and 21203175).

REFERENCES

(1) O'Regan, B.; Grätzel, M. *Nature* **1991**, *353*, 737.

(2) (a) Ardo, S.; Meyer, G. J. *Chem. Soc. Rev.* **2009**, *38*, 115. (b) Bai, Y.; Mora-Seró, I.; De Angelis, F.; Bisquert, J.; Wang, P. *Chem. Rev.* **2014**, *114*, 10095.

(3) For selected examples, see (a) Wang, P.; Zakeeruddin, S. M.; Moser, J.-E.; Nazeeruddin, M. K.; Sekiguchi, T.; Grätzel, M. *Nat. Mater.* **2003**, *2*, 402. (b) Wang, P.; Klein, C.; Humphry-Baker, R.; Zakeeruddin, S. M.; Grätzel, M. *J. Am. Chem. Soc.* **2005**, *127*, 808. (c) Kuang, D.; Klein, C.; Ito, S.; Moser, J.-E.; Humphry-Baker, R.; Evans, N.; Duriaux, F.; Grätzel, C.; Zakeeruddin, S. M.; Grätzel, M. *Adv. Mater.* **2007**, *19*, 1133. (d) Gao, F.; Wang, Y.; Shi, D.; Zhang, J.; Wang, M.; Jing, X.; Humphry-Baker, R.; Wang, P.; Zakeeruddin, S. M.; Grätzel, M. *J. Am. Chem. Soc.* **2008**, *130*, 10720. (e) Chen, C.-Y.; Wang, M.; Li, J.-Y.; Pootrakulchote, N.; Alibabaei, L.; Ngoc-le, C.-h.; Decoppet, J.-D.; Tsai, J.-H.; Grätzel, C.; Wu, C.-G.; Zakeeruddin, S. M.; Grätzel, M. *ACS Nano* **2009**, *3*, 3103.

(4) For selected examples, see (a) Bessho, T.; Zakeeruddin, S. M.; Yeh, C.-Y.; Diau, E. W.-G.; Grätzel, M. *Angew. Chem., Int. Ed.* **2010**, *49*, 6646. (b) Yella, A.; Lee, H.-W.; Tsao, H. N.; Yi, C.; Chandiran, A. K.; Nazeeruddin, M. K.; Diau, E. W.-G.; Yeh, C.-Y.; Zakeeruddin, S. M.; Grätzel, M. *Science* **2011**, *334*, 629. (c) Yella, A.; Mai, C.-L.; Zakeeruddin, S. M.; Chang, S.-N.; Hsieh, C.-H.; Yeh, C.-Y.; Grätzel, M. *Angew. Chem., Int. Ed.* **2014**, *53*, 2973. (d) Mathew, S.; Yella, A.; Gao, P.; Humphry-Baker, R.; Curchod, B. F. E.; Ashari-Astani, N.; Tavernelli, I.; Rothlisberger, U.; Nazeeruddin, M. K.; Grätzel, M. *Nat. Chem.* **2014**, *6*, 242. Selected reviews include (e) Griffith, M. J.; Sunahara, K.; Wagner, P.; Wagner, K.; Wallace, G. G.; Officer, D. L.; Furube, A.; Katoh, R.; Mori, S.; Mozer, A. J. *Chem. Commun.* **2012**, *48*, 4145. (f) Li, L.-L.; Diau, E. W.-G. *Chem. Soc. Rev.* **2013**, *42*, 291. (g) Urbani, M.; Grätzel, M.; Nazeeruddin, M. K.; Torres, T. *Chem. Rev.* **2014**, *114*, 12330. (h) Higashino, T.; Imahori, H. *Dalton Trans.* **2015**, *44*, 448.

(5) For selected reviews, see (a) Mishra, A.; Fischer, M. K. R.; Bäuerle, P. *Angew. Chem., Int. Ed.* **2009**, *48*, 2474. (b) Imahori, H.; Umeyama, T.; Ito, S. *Acc. Chem. Res.* **2009**, *42*, 1809. (c) Clifford, J. N.; Martínez-Ferrero, E.; Viterisi, A.; Palomares, E. *Chem. Soc. Rev.* **2011**, *40*, 1635. (d) Uemura, Y.; Mori, S.; Hara, K.; Koumura, N. *Chem. Lett.* **2011**, *40*, 872. (e) Yen, Y.-S.; Chou, H.-H.; Chen, Y.-C.; Hsu, C.-Y.; Lin, J. T. *J. Mater. Chem.* **2012**, *22*, 8734. (f) Wu, Y.; Zhu, W. *Chem. Soc. Rev.* **2013**, *42*, 2039. (g) Liang, M.; Chen, J. *Chem. Soc. Rev.* **2013**, *42*, 3453.

(6) Zhang, M.; Wang, Y.; Xu, M.; Ma, W.; Li, R.; Wang, P. *Energy Environ. Sci.* **2013**, *6*, 2944.

(7) Kakiage, K.; Aoyama, Y.; Yano, T.; Otsuka, T.; Kyomen, T.; Unno, M.; Hanaya, M. *Chem. Commun.* **2014**, *50*, 6379.

(8) Koumura, N.; Wang, Z.-S.; Mori, S.; Miyashita, M.; Suzuki, E.; Hara, K. *J. Am. Chem. Soc.* **2006**, *128*, 14256.

(9) Würther, F. *Chem. Commun.* **2004**, 1564.

(10) For a comprehensive review, see (a) Li, C.; Wonneberger, H. *Adv. Mater.* **2012**, *24*, 613. For selected examples, see (b) Ferrere, S.; Zaban, A.; Gregg, B. A. *J. Phys. Chem. B* **1997**, *101*, 4490. (c) Ferrere, S.; Gregg, B. A. *New J. Chem.* **2002**, *26*, 1155. (d) Shibano, Y.; Umeyama, T.; Matano, Y.; Imahori, H. *Org. Lett.* **2007**, *9*, 1971. (e) Zafer, C.; Kus, M.; Turkmen, G.; Dincalp, H.; Demic, S.; Kuban, B.; Teoman, Y.; Icli, S. *Sol. Energy Mater. Sol. Cells* **2007**, *91*, 427. (f) Edvinsson, T.; Li, C.; Pschirer, N.; Schöneboom, J.; Eickemeyer, F.; Sens, R.; Boschloo, G.; Herrmann, A.; Müllen, K.; Hagfeldt, A. *J. Phys. Chem. C* **2007**, *111*, 15137. (g) Fortage, J.; Séverac, M.; Houarner-Rassin, C.; Pellegrin, Y.; Blart, E.; Odobel, F. *J. Photochem. Photobiol., A* **2008**, *197*, 156. (h) Jin, Y.; Hua, J.; Wu, W.; Ma, X.; Meng, F. *Synth. Met.* **2008**, *158*, 64. (i) Li, C.; Yum, J.-H.; Moon, S.-J.; Herrmann, A.; Eickemeyer, F.; Pschirer, N. G.; Erk, P.; Schöneboom, J.; Müllen, K.; Grätzel, M.; Nazeeruddin, M. K. *ChemSusChem* **2008**, *1*, 615. (j) Cappel, U. B.; Karlsson, M. H.; Pschirer, N. G.; Eickemeyer, F.; Schöneboom, J.; Erk, P.; Boschloo, G.; Hagfeldt, A. *J. Phys. Chem. C* **2009**, *113*, 14595. (k) Li, C.; Liu, Z.; Schöneboom, J.; Eickemeyer, F.; Pschirer, N. G.; Erk, P.; Herrmann, A.; Müllen, K. *J. Mater. Chem.* **2009**, *19*, 5405. (l) Mathew, S.; Imahori, H. *J. Mater. Chem.* **2011**, *21*, 7166. (m) Keerthi, A.; Liu, Y.; Wang, Q.; Valiyaveettil, S. *Chem.—Eur. J.* **2012**, *18*, 11669. (n) Yao, Z.; Yan, C.; Zhang, M.; Li, R.; Cai, Y.; Wang, P. *Adv. Energy Mater.* **2014**, *4*, 1400244. (o) Zhang, M.; Yao, Z.; Yan, C.; Cai, Y.; Ren, Y.; Zhang, J.; Wang, P. *ACS Photonics* **2014**, *1*, 710. (p) Yan, C.; Ma, W.; Ren, Y.; Zhang, M.; Wang, P. *ACS Appl. Mater. Interfaces* **2015**, *7*, 801. (q) Yang, L.; Ren, Y.; Yao, Z.; Yan, C.; Ma, W.; Wang, P. *J. Phys. Chem. C* **2015**, *119*, 980. (r) Qi, Q.; Wang, X.; Fan, L.; Zheng, B.; Zeng, W.; Luo, J.; Huang, K.-W.; Wang, Q.; Wu, J. *Org. Lett.* **2015**, *17*, 724.

(11) Luo, J.; Xu, M.; Li, R.; Huang, K.-W.; Jiang, C.; Qi, Q.; Zeng, W.; Zhang, J.; Chi, C.; Wang, P.; Wu, J. *J. Am. Chem. Soc.* **2014**, *136*, 265.

(12) Yao, Z.; Wu, H.; Ren, Y.; Guo, Y.; Wang, P. *Energy Environ. Sci.* **2015**, DOI: 10.1039/c4ee03934c.

(13) (a) Li, R.; Liu, J.; Cai, N.; Zhang, M.; Wang, P. *J. Phys. Chem. B* **2010**, *114*, 4461. (b) Cai, N.; Li, R.; Wang, Y.; Zhang, M.; Wang, P. *Energy Environ. Sci.* **2013**, *6*, 139. (c) Yao, Z.; Yang, L.; Cai, Y.; Yan, C.; Zhang, M.; Cai, N.; Dong, X.; Wang, P. *J. Phys. Chem. C* **2014**, *118*, 2977.

(14) Hagfeldt, A.; Boschloo, G.; Sun, L.; Kloo, L.; Pettersson, H. *Chem. Rev.* **2010**, *110*, 6595.

(15) Tietze, L. F.; Brasche, G.; Grube, A.; Böhnke, N.; Stadler, C. *Chem.—Eur. J.* **2007**, *13*, 8543.

(16) Matthews, C. J.; Leese, T. A.; Thorp, D.; Lockhart, J. C. *J. Chem. Soc., Dalton Trans.* **1998**, 79.

(17) Jiang, W.; Qian, H.; Li, Y.; Wang, Z. *J. Org. Chem.* **2008**, *73*, 7369.

(18) Becke, A. D. *J. Chem. Phys.* **1993**, *98*, 1372.

(19) (a) Lynch, B. J.; Fast, P. L.; Harris, M.; Truhlar, D. G. *J. Phys. Chem. A* **2000**, *104*, 4811. (b) Pastore, M.; Mosconi, E.; De Angelis, F.; Grätzel, M. *J. Phys. Chem. C* **2010**, *114*, 7205.

(20) Cossi, M.; Rega, N.; Scalmani, G.; Barone, V. *J. Comput. Chem.* **2003**, *24*, 669.

(21) (a) Qu, P.; Meyer, G. J. *Langmuir* **2001**, *17*, 6720. (b) Santos, T. D.; Morandeira, A.; Koops, S.; Mozer, A. J.; Tsekouras, G.; Dong, Y.; Wagner, P.; Wallace, G.; Earles, J. C.; Gordon, K. C.; Officer, D.; Durrant, J. R. *J. Phys. Chem. C* **2010**, *114*, 3276.

(22) (a) Feldt, S. M.; Gibson, E. A.; Gabrielsson, E.; Sun, L.; Boschloo, G.; Hagfeldt, A. *J. Am. Chem. Soc.* **2010**, *132*, 16714. (b) Zhou, D.; Yu, Q.; Cai, N.; Bai, Y.; Wang, Y.; Wang, P. *Energy Environ. Sci.* **2011**, *4*, 2030.

(23) Furube, A.; Wang, Z.-S.; Sunahara, K.; Hara, K.; Katoh, R.; Tachiya, M. *J. Am. Chem. Soc.* **2010**, *132*, 6614.

(24) (a) O'Regan, B. C.; Durrant, J. R. *Acc. Chem. Res.* **2009**, *42*, 1799. (b) Fabregat-Santiago, F.; Garcia-Belmonte, G.; Mora-Seró, I.; Bisquert, J. *Phys. Chem. Chem. Phys.* **2011**, *13*, 9083. (c) Clifford, J. N.; Martínez-Ferrero, E.; Polomares, E. *J. Mater. Chem.* **2012**, *22*, 12415.

(25) Duffy, N. W.; Peter, L. M.; Rajapakse, R. M. G.; Wijayant, K. G. U. *Electrochem. Commun.* **2000**, *2*, 658.

(26) O'Regan, B. C.; Scully, S.; Mayer, A. C.; Palomares, E.; Durrant, J. *J. Phys. Chem. B* **2005**, *109*, 4616.

(27) Wang, Y.; Yang, L.; Zhang, J.; Li, R.; Zhang, M.; Wang, P. *ChemPhysChem* **2014**, *15*, 1037.

DOI: 10.1021/jacs.5b01537
J. Am. Chem. Soc. 2015, 137, 3799−3802